

**Extracellular vesicle-mediated co-delivery of TRAIL and Dinaciclib for targeted  
therapy of resistant tumor**

Changhong Ke<sup>2,#</sup>, Huan Hou<sup>1,#</sup>, Kui Su<sup>1,#</sup>, Chaohong Huang<sup>1</sup>, Qian Yuan<sup>1</sup>, Shuyi Li<sup>1</sup>, Jianwu Sun<sup>1</sup>, Yue Lin<sup>1</sup>, Chuanbin Wu<sup>2</sup>, Yu Zhao<sup>1,\*</sup>, Zhengqiang Yuan<sup>1,\*</sup>

1.School of Biomedical and Pharmaceutical Sciences, Guangdong University of Technology,  
Guangzhou 510006, China

2. School of Pharmacy, Jinan University, Guangzhou 510632, China

#: These authors contributed equally to this study.

## Supplementary Figures

### Figure S1

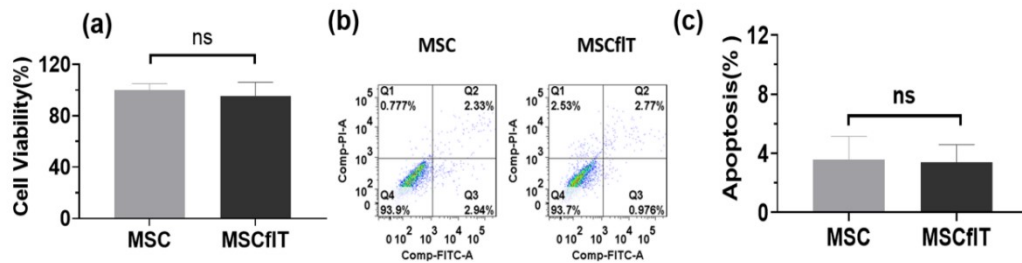


**Figure S1. MSC viability is not affected by TRAIL transduction.** (a) Comparison of cellular viability and proliferation between MSC and MSCfIT cells. Cells were cultured to 70% confluency, then assessed for cellular viability by using the Cell Counting Kit 8 (CCK-8); (b). Apoptosis assay of MSC and MSCfIT cells by FITC-Annexin-V/PI labeling combined with flow cytometry analysis. (c). Comparison of apoptosis rates of MSCs and MSCfITs. ns, not significant, by Student's t test.

### Figure S2

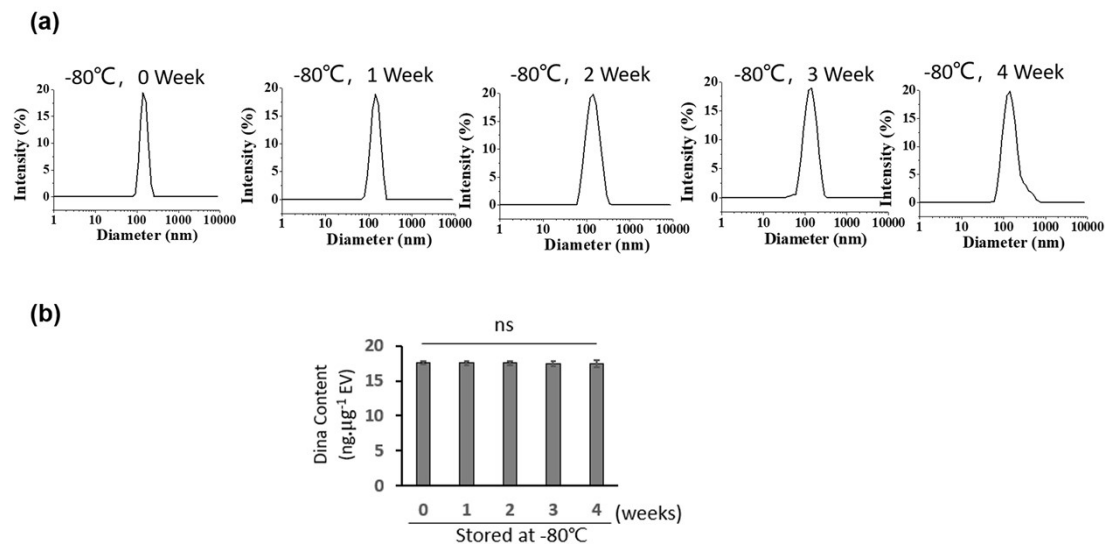


**Figure S2. Examination of physical stability of Dina@EV-Ts during storage at -80°C.** Aliquots of Dina@EV-Ts with a Dina content as 17.6 ng·µg<sup>-1</sup> EV-T were frozen at -80°C for 0-4 weeks first, then thawed and analyzed for particle size and Dina content, respectively. (a) Particle size analysis by Dynamic Light Scattering (Malvern); (b) Assessment of Dina content

by a UV spectrometer at 255 nm. Samples were tested in triplicates and the data were presented as mean  $\pm$  SD (n=3). ns, not significant, versus 0-week control by student's t-test.

**Figure S3**

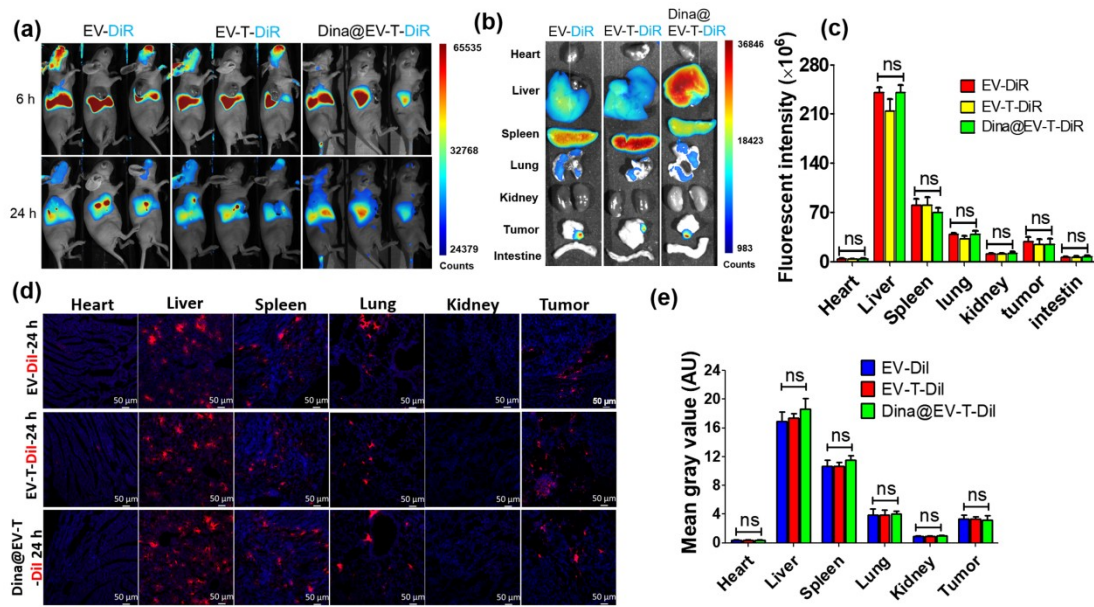


**Figure S3. Comparison of in vivo biodistribution of systemically infused EVs, EV-Ts and Dina@EV-Ts in subcutaneous A549 xenograft tumor-bearing mice.** (a) Examination of biodistribution of DiR labeled EVs, EV-Ts and Dina@EV-Ts in systemically administered tumor-bearing nude mice at 6 h and 24 h, respectively, by an in vivo imaging system (IVIS). (b) Biodistribution of DiR labeled EVs, EV-Ts and Dina@EV-Ts in isolated animal organs and tumours examined by IVIS. (c) Quantification and comparison of DiR signal intensity in organs and tumors by IVIS. (d) Examination of DiI biodistribution in isolated animal organs and tumours by fluorescent confocal microscopy. DiI labeled EVs (EV-DiI), EV-Ts (EV-T-DiI) or Dina@EV-T (Dina@EV-T-DiI) were *i.v.* infused in subcutaneous A549 tumor-bearing mice, and after 24 h, animals were sacrificed and organs (heart, liver, spleen, lung and kidney) and tumours were collected and cryo-sectioned and stained by DAPI, followed by confocal microscopic imaging and analyses. (e) Quantification and comparison of DiI signal intensity in organs and tumors by measuring integrated DiI labeling density per selected area using Image J software. All values are means  $\pm$  SD (n=6), ns, not significant, by one-way ANOVA/Bonferroni multiple comparison post hoc test.

**Figure S4**

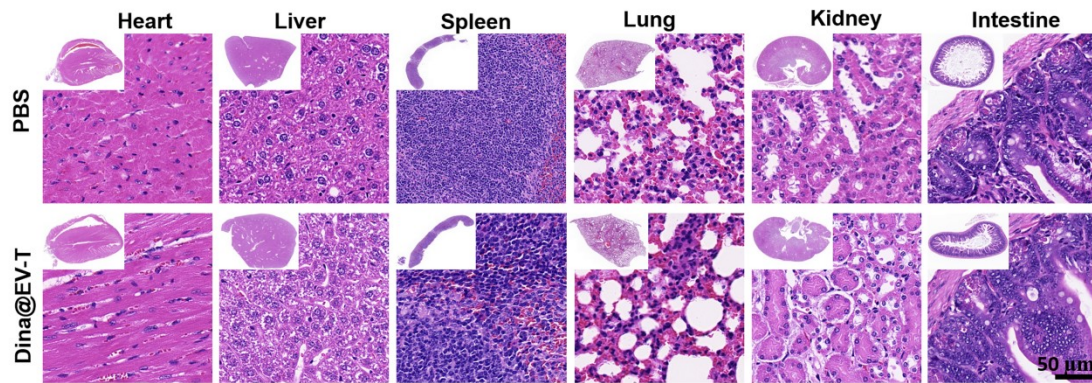


**Figure S4. H&E staining of mice organs.** Animal organs including heart, lung, liver, spleen, kidney and intestine were collected and stained by H&E to check any sign of adverse side effects at the experimental endpoints from mice treated by saline control (PBS) or Dina@EV-T as described in Figure 6b. The corner insets illustrate gross view of tissue sections while the big pictures show the microscopic view.

**Figure S5**

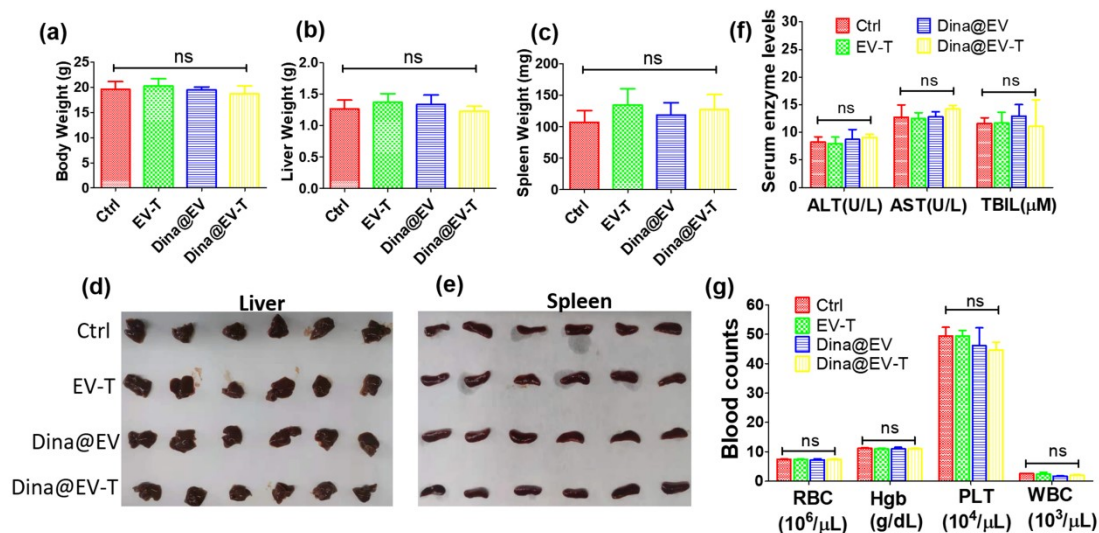


**Figure S5. Examination of effects of therapeutic agents on liver function and blood cell counts in subcutaneous A549 xenograft tumor-bearing nude mice.** Tumor-bearing Balb/c nude mice were intravenously infused with vehicle control (Ctrl), EV-T, Dina@EV and Dina@EV-T, respectively, with the same treatment regime described in Fig. 6a-b. Twenty-four hours post the last treatment, mice were measured for body weight (a) first, then culled, livers

and spleens isolated and weighted (b-c), and photographed (d-e); moreover, animal blood samples were also collected for measurement of serum levels of alanine (ALT) and aspartate (AST) aminotransferases, and total bilirubin (TBIL) (f), and also for hematological analyses of haemoglobin (Hgb) level and blood cell counting including red blood cell (RBC), white blood cell (WBC) and platelet (PLT) (g). All values are means  $\pm$  SD (n=6), ns, not significant, by Student's t test. There were no significant measurement differences among four examined treatment groups.

**Figure S6**

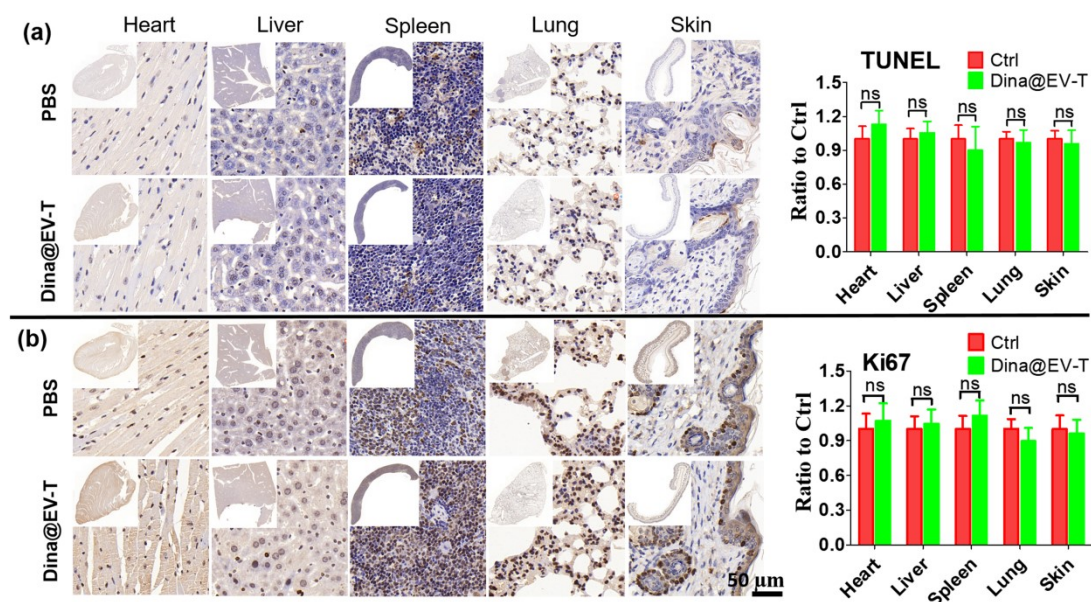


**Figure S6. Immunohistochemistry (IHC) analyses of animal organs and skin.**

Subcutaneous A549 xenograft tumor-bearing Balb/c nude mice were treated by vehicle control (PBS) or Dina@EV-T as described in Fig. 6. At the experimental endpoints, mice organs (heart, liver, spleen and lung) and skin tissues were collected and stained for cellular proliferation maker Ki-67 and apoptosis (TUNEL), respectively, to check any likely adverse side effects. The corner insets illustrate gross view of tissue sections while the big pictures show the microscopic view. (a) TUNEL assay. (b) Ki-67 staining. Ten histologically similar fields were selected for quantification on each sample and the Image-pro plus 6.0 software was used to quantitatively analyze the slides. Quantification of IHC positive staining signal intensity is shown relative to vehicle control for which the value was set as 1.0. All values are means  $\pm$  SD

(n=10), ns, not significant, by Student's t test.